

# Density functional theory studies of the adsorption of hydrogen sulfide on aluminum doped silicane

Francisco Sánchez-Ochoa · Jonathan Guerrero-Sánchez · Gabriel I. Canto · Gregorio H. Coccoletzi · Noboru Takeuchi

Received: 19 February 2013 / Accepted: 30 April 2013 / Published online: 22 May 2013  
© Springer-Verlag Berlin Heidelberg 2013

**Abstract** First principles total energy calculations have been performed to study the hydrogen sulfide ( $H_2S$ ) adsorption on silicane, an unusual one monolayer of Si(111) surface hydrogenated on both sides. The  $H_2S$  adsorption may take place in dissociative or non-dissociative forms. Silicane has been considered as: (A) non-doped with a hydrogen vacancy, and doped in two main configurations; (B) with an aluminum replacing a hydrogen atom and (C- $n$ ;  $n=1, 2, 3$ ) with an aluminum replacing a silicon atom at a lattice site. In addition, three supercells;  $4 \times 4$ ,  $3 \times 3$  and  $2 \times 2$  have been explored for both non-doped and doped silicane. The non-dissociative adsorption takes place in geometries (A), (C-1), (C-2) and (C-3) while the dissociative in (B). Adsorption energies of the dissociative case are larger than those corresponding to the non-dissociated cases. In the dissociative adsorption, the molecule is fragmented in a HS structure and a H atom which are bonded to the aluminum to form a H-S-Al-H structure. The presence of the doping produces some electronic changes as the periodicity varies. Calculations of the total density of states (DOS) indicate that in most cases

the energy gap decreases as the periodicity changes from  $4 \times 4$  to  $2 \times 2$ . The features of the total DOS are explained in terms of the partial DOS. The reported charge density plots explain quite well the chemisorptions and physisorptions of the molecule on silicane in agreement with adsorption energies.

**Keywords** Al-doped silicane · Charge density · First principles calculations · Hydrogen sulfide · Partial density of states · Silicane · Total density of states

## Introduction

Interactions of hydrogen sulfide ( $H_2S$ ) with semiconductor and metallic surfaces have been intensively investigated theoretically and experimentally [1–3] in the past few years due to the possible applications of these systems in sensor devices, electronics, catalysis and electrolysis. Hydrogen sulfide is a gas contained in many natural and synthetic processes as in crude petroleum, natural gas, and hot springs.  $H_2S$  is produced by bacterial breakdown of organic materials, human and animal wastes (e.g., sewage). The molecule is also a byproduct in many metallurgical processes and is a major pollutant in the environment. Thus, the development of  $H_2S$  sensors has been an active field of study for a long time [4, 5]. It is noteworthy that the sulfidation process, similar to oxidation, is a corrosive process that affects properties of materials, such as steel [6]. Sulfidation can also be used to passivate chemically reactive surfaces, such as those of GaAs and Si [7]. Theoretical [8, 9] and experimental [10] studies have been performed to investigate the  $H_2S$  adsorption on Fe(110), Pt(111), Ge(001) and Si (001)(011)(111) surfaces. High resolution electron energy loss spectroscopy (HREELS) and scanning tunneling microscopy (STM)

F. Sánchez-Ochoa (✉) · J. Guerrero-Sánchez · G. H. Coccoletzi  
Instituto de Física “Ing. Luis Rivera Terrazas”, Benemérita  
Universidad Autónoma de Puebla, Puebla, Mexico  
e-mail: fsanchez@ifuap.buap.mx

J. Guerrero-Sánchez  
e-mail: guerrero@ifuap.buap.mx

G. H. Coccoletzi  
e-mail: coccoletz@ifuap.buap.mx

G. I. Canto  
Centro de Investigación en Corrosión, Universidad Autónoma  
de Campeche, Campeche, Mexico  
e-mail: gcanto@uacam.mx

N. Takeuchi  
Centro de Nanociencias y Nanotecnología, Universidad Nacional  
Autónoma de México, Mexico, Mexico  
e-mail: takeuchi@cny.n.unam.mx

[11–13] studies have been recently done on the interaction of hydrogen sulfide with silicon surfaces. As it stands the detection and conversion of H<sub>2</sub>S to other chemicals is essential for a healthy environment and a safe industry.

Most of the above described works deal with surfaces of materials however there exists a great interest in exploring two dimensional systems such as graphene. It is also currently attractive for the study of materials with graphene-like crystal structure [14, 15], where the atomic configuration is composed by the sp<sup>2</sup> hybridization. Two dimensional layers have striking properties, which lead to potentially novel applications [14–16] however the coupling with electronic devices is still an open problem. In this work is addressed the study of the H<sub>2</sub>S adsorption on silicane, which displays electronic configurations similar to those of graphane (CH); this 2D-dimensional system may be considered as a good candidate for H<sub>2</sub> storage [17, 18].

Silicene, a graphene-like system, is a substance composed of pure silicon, with atoms arranged in a regular hexagonal pattern similar to graphite, but in a one-atom thick sheet. Similar to graphane, silicane [19–21] is a form of hydrogenated silicene. Silicene has been studied both theoretical [16, 22–24] and experimentally [25–27] since this system may be applied in the electronic industry, as it displays singular chemical and physical properties. Theoretical studies based on the density functional theory (DFT) and the tight-binding approach have been developed to investigate the properties of this prominent material with results showing that the most stable configuration is non-planar [23, 28] where the nearest neighbors atoms alternate between two planes with a small separation, in a low buckled honeycomb sheet. The explanation of why carbon makes honeycomb structures but silicon does not stems from the fact that in carbon the sp<sup>2</sup> hybridization is more stable than sp<sup>3</sup>, but in silicon this is reversed. Silicene has been determined to be a zero-gap semiconductor with massless Dirac fermions, similar to graphene. Studies show that silicene layers passivated with hydrogen exhibit an indirect band gap, of energy  $E_{gap,ind}(\Gamma-M) \cong 2.2$  eV, emerging at the  $\Gamma$  point and with transitions to the M point [21]; this indicates that the electronic properties of silicene can be modified by partial or complete hydrogenation [22–24]. The hydrosilicon honeycomb structure is termed silicane (Si<sub>2</sub>H<sub>2</sub>). Due to the high reactivity compared with graphene, the adsorption of atoms on the silicane surface can lead to a more stable semiconductor. Thus, the presence of adsorbed elements on the surface or like impurities in the lattice will change the silicane properties [29]. Detecting changes in the electrical conductivity of silicene produced by the adsorption of atoms or molecules it is possible to sense particles in the atmosphere. Hence silicane may be used in gas sensor devices, among other possible optoelectronic applications as suggested in the literature [29–31]. Surprisingly this H-saturated Si layer was synthesized a long time ago in the form

of layered polysilane [32, 33], however little effort has been done to explore the interactions of molecules with this layer. Here ab-initio calculations are performed to investigate the H<sub>2</sub>S adsorption on silicane considering different configurations. Also, relaxed structures, binding energies, total density of states (DOS), partial density of states (PDOS) and charge density plots are calculated. The study is interesting provided that in this way it is possible to explore the possible H<sub>2</sub>S or S storage in an efficient and controllable adsorption/desorption system.

## Computational framework

To investigate the interaction of H<sub>2</sub>S with silicane and Al doped silicane, first principles total energy calculations are performed within the periodic density functional theory as implemented in the SIESTA code [34, 35]. Calculations consider silicane [22–24] as one monolayer of Si(111) surface hydrogenated on both sides in supercell periodicities: 4x4, 3x3 and 2x2. Different supercells allow dealing with variations of H<sub>2</sub>S and doping element concentrations, see panel (a) of Fig. 1. Several initial molecule orientations are taken into account when placing the molecule on the silicane surface. In the first place, the interaction of the hydrogen sulfide with the silicane in the presence of a hydrogen vacancy is investigated. Then the doping with Al is explored by placing the element at different sites; in one case the Al is at a hydrogen site and in the other at a silicane lattice site.

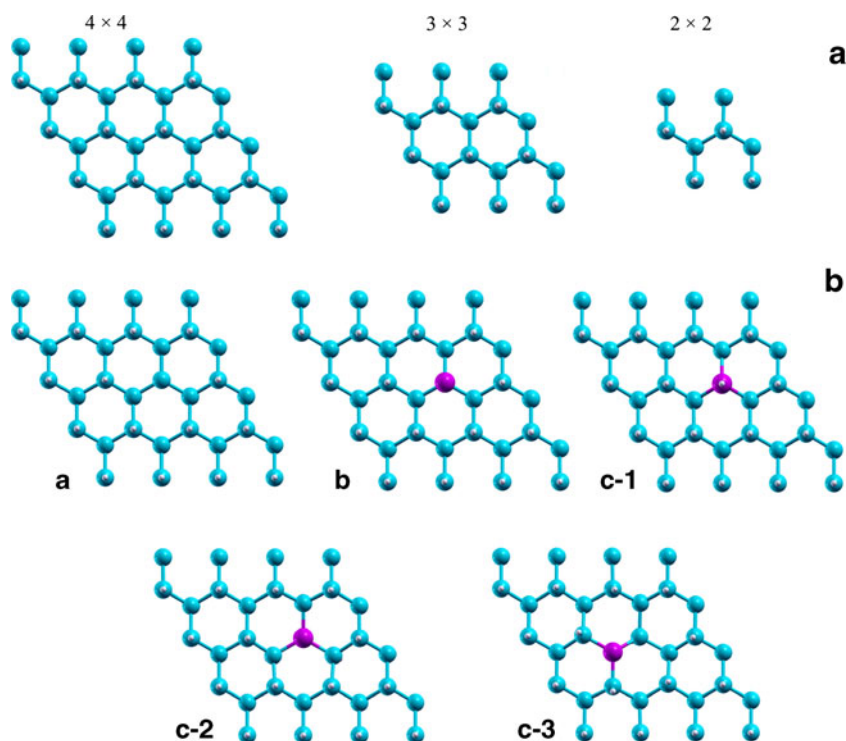
The electron states are expanded in a linear combination of atomic orbitals (LCAO). The exchange and correlation energies are treated according to the generalized gradient approximation (GGA) within the Perdew, Burke and Enzerhoff (PBE) [36] formalism. To deal with the electron-ion interactions the norm-conserving pseudopotentials [37, 38] are employed, in their fully nonlocal form [39]. A double zeta polarized (DZP) basis set has been used [40]. To prevent any interaction between two adjacent supercells a vacuum gap greater than 15 Å is used in the direction perpendicular to the silicane layer. Brillouin-zone integrations are done using special k-point according to the Monkhorst-Pack scheme [41], with a mesh resolution of  $2\pi \times 0.5$  Å<sup>-1</sup>. The structure relaxations have been performed with meshcutoff energy of 350 Ry. To study the electronic properties the k-points meshes are increased to 21×21×1, 31×31×1, and 41×41×1 for the 4x4, 3x3 and 2x2 periodicities, respectively.

## Results and discussion

### Structural properties

This section is devoted to presenting results of the dissociative and non dissociative interactions of H<sub>2</sub>S with silicane

**Fig. 1** Panel **a** shows the silicane in three different periodicities, 4x4, 3x3 and 2x2. **b** displays silicane in different configurations: (A) with a hydrogen vacancy; (B) the Al replacing one H; (C-1) the aluminum replacing a silicon at the upper monolayer, with a H attached to the Al; (C-2) the aluminum replacing a silicon at the upper silicane monolayer with no hydrogen; (C-3) the aluminum replacing a silicon at the lower silicane monolayer with no hydrogen. (The Al concentration increases from 4x4 to 2x2)



and aluminum doped silicane. Calculations start with the geometry optimization of the silicane structure with periodicities 4x4, 3x3 and 2x2 containing 64, 36 and 18 Si atoms, respectively. A schematic example is presented in Fig. 1(a). Silicane with a hydrogen vacancy (geometry A) is depicted in panel (b) of Fig. 1. The doping by aluminum has been explored in two geometries; in the first case by replacing one saturating H by one Al (configuration B of Fig. 1b) and in the second replacing one Si by one Al (configurations C-1, C-2 and C-3 of Fig. 1b). The aluminum concentrations are 3.125, 5.55 and 12.5 % for the 4x4, 3x3 and 2x2 periodicities, respectively. To determine the most stable geometries different orientations of the H<sub>2</sub>S molecule with respect to the silicane plane are explored.

H<sub>2</sub>S has a tetrahedral arrangement of electron pairs with two bonding pairs and two lone pairs having bent geometry. The isolated molecule displays a dipole moment of 0.97 D. Results of the calculated structural parameters of the H<sub>2</sub>S are: the bond angle (H-S-H), 91.66° and the S-H bond length, 1.358 Å, which are in agreement with those reported: the angle, 92.07° and bond length, 1.335 Å, these were determined using experimental measurements [42]. On the other hand, reported silicane structural parameters calculated within the DFT formalism [14–16] show differences with those of bulk silicon. The silicane bond length,  $d_{\text{Si-Si}}$  is 2.35 Å, is contracted by about 0.03 Å, this leads to a  $sp^3$ -like hybridization. Moreover, the Si-H bonds are weakly polarized (partial electron transfer of about 0.1|e| from Si to H atoms), inducing only a slightly polarized surface.

Experimental evidences have demonstrated the adsorption of dissociated H<sub>2</sub>S molecules to form H and HS structures on the Si (100) surface [43]. A DFT work has been reported on the dissociative adsorption of H<sub>2</sub>S on metals and transition metals [44]. The dissociated fragments SH and H share the smallest number of surface metal atoms (principle of least atom sharing). Therefore it is interesting to investigate the formation of atomic structures after H<sub>2</sub>S dissociative adsorption on silicane.

#### Geometry A

The non dissociative interaction of the hydrogen sulfide with silicane in the presence of a hydrogen vacancy, termed as geometry A, is described in this section, see panel (b) of Fig. 1. The 4x4 periodicity is first described. The most stable structure is obtained when the H<sub>2</sub>S interacts with the silicane at the vicinity of the vacancy site. The molecule plane is perpendicular to the silicane plane. One of the hydrogen atoms of the H<sub>2</sub>S interacts directly with the unsaturated silicon atom at a distance of 2.11 Å. The H-S-H angle is 90.7°, a lateral view is shown in (A) of Fig. 2. In the 3x3 periodicity the adsorption occurs again with the molecule plane being perpendicular to the silicane layer. Similar to the previous case one of the hydrogen atoms interacts directly with the unsaturated silicon atom at a distance of 2.17 Å. The H-S-H angle is 90.5°. The 2x2 periodicity shows similar atomic structure as those of the 4x4 and 3x3. The hydrogen atom of the molecule which is

interacting directly with the unsaturated silicon atom is at a distance of 2.21 Å. The H-S-H angle is 90.6°. Small changes are obtained as the supercell size decreases, the interaction distance increases slightly which reduces.

### Geometry B

Panel (b) of Fig. 1 shows the aluminum doped silicane. In this configuration the aluminum replaces the hydrogen this is termed as geometry B. Results of the dissociated adsorption of H<sub>2</sub>S on the doped silicane in 4x4-periodicity are described in what follows. Various initial orientations of the H<sub>2</sub>S are taken into account. At the energy minimum the molecule forms structures with the aluminum: H-S-Al-H. The HS fragment and the hydrogen atom are bonded to the doping Al atom, making two possible configurations. In the first the H bonded to the S is pointing toward the silicane surface. The H-S-Al form an angle of 94.3° and the S-Al-H

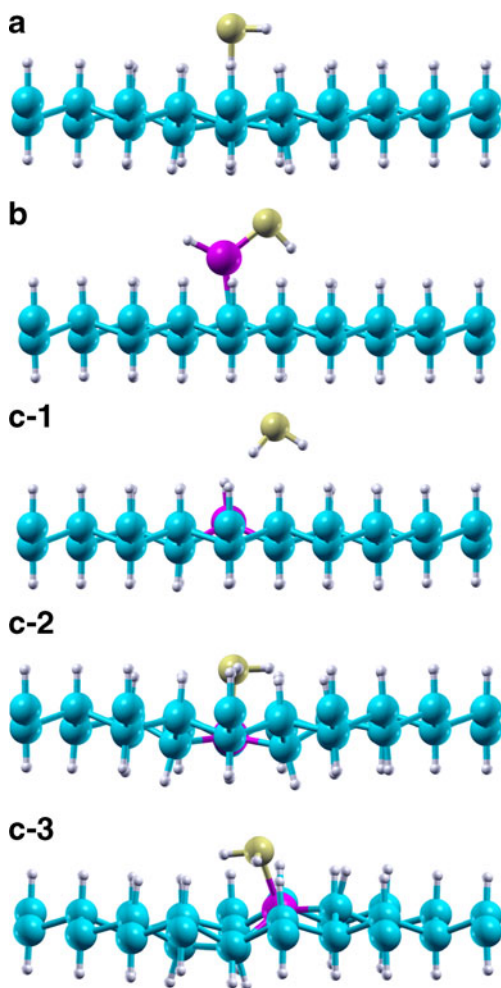


**Fig. 2** The figure exhibits the most stable structures of the interaction of H<sub>2</sub>S with silicane: **a** with a vacancy of hydrogen; **b** in the non-dissociative geometry; (C-1) dissociative geometry, (C-2) and (C-3) in the non-dissociative configurations

displays an angle of 114.8°, with the S-Al bond length of 2.19 Å. In the second geometry the H bonded to the S is pointing outward of the silicane surface. The H-S-Al displays an angle of 92.5° and the S-Al-H an angle of 118°, with the S-Al bond length of 2.19 Å. The total energy of the former configuration exhibits the lowest minimum consequently this is taken as the ground state, a lateral view is shown in (B) of Fig. 2. The increase in the aluminum and hydrogen sulfide concentrations produce only small changes in the structure. Both angles H-S-Al and S-Al-H experience small variations with respect to the 4x4 periodicity.

### Geometry C-1

In geometry C-1 shown in panel (b) of Fig. 1 the aluminum atom replaces a silicon atom of the silicane upper monolayer, with the hydrogen attached to the aluminum atom. The non dissociated H<sub>2</sub>S molecule is placed on top of the silicane. The structure is somewhat distorted as compared with the non doped structure. Studies of the 4x4 periodicity are described. In the most stable configuration the adsorption takes place on the silicane surface with the hydrogen atoms of the molecule pointing toward the silicane. The H-S-H angle has the value of 91.7°, a lateral view is shown in (C-1) of Fig. 2. The 3x3 periodicity shows similar configurations the molecule interacts with the silicane through the hydrogen atoms. The H-S-H angle has the value of 92°. In the 2x2 periodicity similar results were obtained. The H-S-H angle has the value of 91.3°.

### Geometry C-2

Results of geometry C-2 are described in this section. In this geometry an aluminum atom replaces a silicon atom of the upper monolayer with no hydrogen attached to it, see panel (b) of Fig. 1. The aluminum is surrounded by saturated silicon atoms in the upper monolayer. In this configuration the adsorption is non dissociative. In the lowest minimum energy the adsorbed H<sub>2</sub>S molecule plane is parallel to the silicane layer, the S bonds to the Al. The low coverage exhibits the S-Al bond length of 2.56 Å and the H-S-H angle of 91.7°, a lateral view is shown in (C-2) of Fig. 2. The intermediate coverage displays the S-Al bond length of 2.55 Å and the H-S-H angle of 92°. In the high coverage the S-Al bond length is 2.56 Å and the H-S-H angle of 91.6°. It is evident that the S-Al bond length is almost unaffected by the change in Al concentration while the molecule angles suffer only small variations.

### Geometry C-3

Geometry C-3 (see panel (b) of Fig. 1) is formed when the doping aluminum is at the lower silicane monolayer initially

with a hydrogen atom bonded to it. The non dissociative adsorption is obtained with the molecule plane being non parallel to the silicane layer. In this configuration the S bonds to the Al. The low coverage exhibits the S-Al bond length of 2.53 Å and the H-S-H angle of 92.10°, a lateral view is shown in (C-3) of Fig. 2. The intermediate coverage displays the S-Al bond length of 2.54 Å and the H-S-H angle of 92.1°. In the high coverage the S-Al bond length is 2.57 Å and the H-S-H angle of 91.3°. Note that the S-Al bond length exhibits a small increase and the molecule angles suffer only small variations as the coverage increases.

### Binding energies

To measure the interaction strength between the H<sub>2</sub>S and the silicane the adsorption energy,  $E_{\text{ads}}$ , is calculated using the formula [45]

$$E_{\text{ads}} = E_{\text{H}_2\text{S}+\text{silicane}} - (E_{\text{silicane}} + E_{\text{H}_2\text{S}}) \quad (1)$$

where  $E_{\text{H}_2\text{S}+\text{silicane}}$  is the total energy of the relaxed H<sub>2</sub>S-silicane system, while  $E_{\text{silicane}}$  and  $E_{\text{H}_2\text{S}}$  are the total energies of the relaxed silicane and the H<sub>2</sub>S molecule, respectively. With this definition, more negative energy values represent stronger interactions between the adsorbed H<sub>2</sub>S and the silicane. It also indicates that the adsorption is exothermic.

Adsorption energies of geometry A are: -0.212, -0.210 and -0.186 eV for the 4x4, 3x3 and 2x2 periodicities, respectively. Values indicate that there is physisorption. Taking into account these energy the system might be suggested as a good candidate to fabricate gas sensor devices. In geometry B the adsorption energies are large indicating chemisorptions, the 2x2 periodicity has the largest adsorption energy; the bond lengths are almost unaffected (this has been discussed in [Introduction](#)); thus, the adsorption energy only shows a small increase with concentration. It may be suggest as the system to study molecular dissociation.

In the replacement of a Si atom by Al at the upper monolayer, termed as geometry C-1, the interaction between H<sub>2</sub>S, and silicane is slightly stronger than that of the H<sub>2</sub>S-Si interaction in geometry A. Recall that geometries C-2 and C-3 contain hydrogen vacancies and Al at a lattice site; in these systems the adsorption energies have similar values. They show chemisorptions. Moreover, C-2 and C-3 display covalent bonds.

Calculations have been done using a GGA functional, which yield underestimated binding energies. In contrast, when the LDA functional is applied binding energies are overestimated [17, 18]. On the other hand, it is known that in some studies on binding energies and formation energies the zero point energy (ZPE) is important and is taken into account; however, in the present studies the approach already published is followed [46] which considers the zero point energy as unimportant. The ZPE corrections do not

improve significantly the calculated values. Therefore, it is unimportant to consider ZPE for the purposes of the present work. A summary of adsorption energies is presented in Table 1.

### Electronic properties

#### *Total density of states (DOS) and partial density of states (PDOS)*

In previous sections the structural properties in different configurations of the interactions between hydrogen sulfide and silicane have been described, in what follows the total density of states and partial DOS to explain the electronic properties is presented. Both non dissociated and dissociated hydrogen sulfide systems are investigated. In addition silicane is considered in one case with a hydrogen vacancy and in the other the silicane is doped.

#### *Geometry A*

The total DOS and partial DOS of the non dissociative interactions of the hydrogen sulfide with silicane in geometry A are first described. In panel (A) of Fig. 3a is displayed the total DOS and in panel (A) of Fig. 3b the partial DOS of the optimal configuration in the 4x4 periodicity. In the figure the energy reference is the Fermi level (dashed line at zero). Note that an energy gap is present with estimated value of 2.25 eV (2.3 and 2.05 eV for the 3x3 and 2x2 periodicities, respectively). When features of the 4x4 case are compared with those corresponding to the 3x3 and 2x2 periodicities only minor structural changes are found with the periodicity. A small energy gap increase is obtained with

**Table 1** The first column labels the five-different structures, in the second column the corresponding periodicities, and in third the adsorption energies  $E_{\text{ads}}$ . Results are reported for the most stable structures

Structure	Periodicity	$E_{\text{ads}}$ [eV]
A	4x4	-0.212
	3x3	-0.210
	2x2	-0.186
B	4x4	-2.965
	3x3	-2.973
	2x2	-3.070
C-1	4x4	-0.240
	3x3	-0.224
	2x2	-0.205
C-2	4x4	-0.835
	3x3	-0.788
	2x2	-0.757
C-3	4x4	-0.770
	3x3	-0.772
	2x2	-0.750

the change in periodicity in going from 4x4 to 3x3 however this is reversed when changing from 3x3 to 2x2. These effects are attributed to the increase in Al concentration. The 4x4 periodicity total DOS features interpretation is given in terms of the partial DOS reported in panel (A) of Fig. 3b. At the valence band the structure is mainly composed of the Si- and S-3p orbitals, and the H-1s orbital. At the conduction band the total DOS is formed by the contributions of the Si-3p and H-1s orbitals, no S orbital is present. In addition there exists a sharp peak at the Fermi level which is composed of the Si- and S-3p orbitals and the H-1s orbital. PDOS corresponding to the 3x3 and 2x2 present similar behavior therefore no figures are reported.

### Geometry B

Results of the DOS and partial DOS corresponding to the dissociated adsorption of H<sub>2</sub>S on silicane doped by Al in configuration B are presented in this section. The total DOS of the lowest minimum energy in the 4x4 periodicity is presented in panel (B) of Fig. 3a and the partial DOS in panel (B) of Fig. 3b. In the figure, the energy reference is the Fermi level (dashed line at zero). Note the presence of an energy gap with estimated value of 2.25 eV (2.2 and 2.15 eV for the 3x3 and 2x2 periodicities, respectively). Comparisons of the 4x4 DOS features with those corresponding to the 3x3 and 2x2 periodicities show minor structural changes with the periodicity. A small energy gap reduction is obtained with the change in periodicity (from 4x4 to 2x2) which is mainly induced by the increase in Al

concentration. The interpretation of the total DOS features is given in terms of the partial DOS presented in panel (B) of Fig. 3b for the 4x4 periodicity. Within the valence band the contributions come from S-3p, Al-3p, Si-3p and H-1s orbitals, with S and Si making the main contributions, nevertheless Al also participates. At the conduction band, the total DOS is mainly formed by the Al-3p and 3s, and Si-3p orbitals. As in geometry A the partial DOS corresponding to the 3x3 and 2x2 periodicities exhibit similar contributions to the total DOS therefore they are not reported.

### Geometry C-1

This section is devoted to describing the density of states in geometry C-1. Results of the total DOS are displayed in panel (C-1) of Fig. 3a and the partial DOS in panel (C-1) of Fig. 3b for the 4x4 periodicity. Note that the Fermi level is in the valence band. The total DOS features exhibit some minor structural changes with the periodicity. One point to remark is that the estimated energy gap decreases as the aluminum concentration increases; from 2.09 eV for the 4x4 to 1.7 eV for the 2x2 supercell. The structural interpretation is given again in terms of the partial DOS. As stated above in panel (C-1) of Fig. 3a the total DOS in the 4x4 periodicity is shown, which is obtained with contributions of S, Al, Si and H orbitals reported in panel (C-1) of Fig. 3b. The valence band is formed by the S-3p, Al-3p, Si-3p and H-1s orbitals, with S and Si making the most important contributions, nevertheless Al-3s orbital and the H-1s orbitals are contributing. At the conduction band, the total DOS is

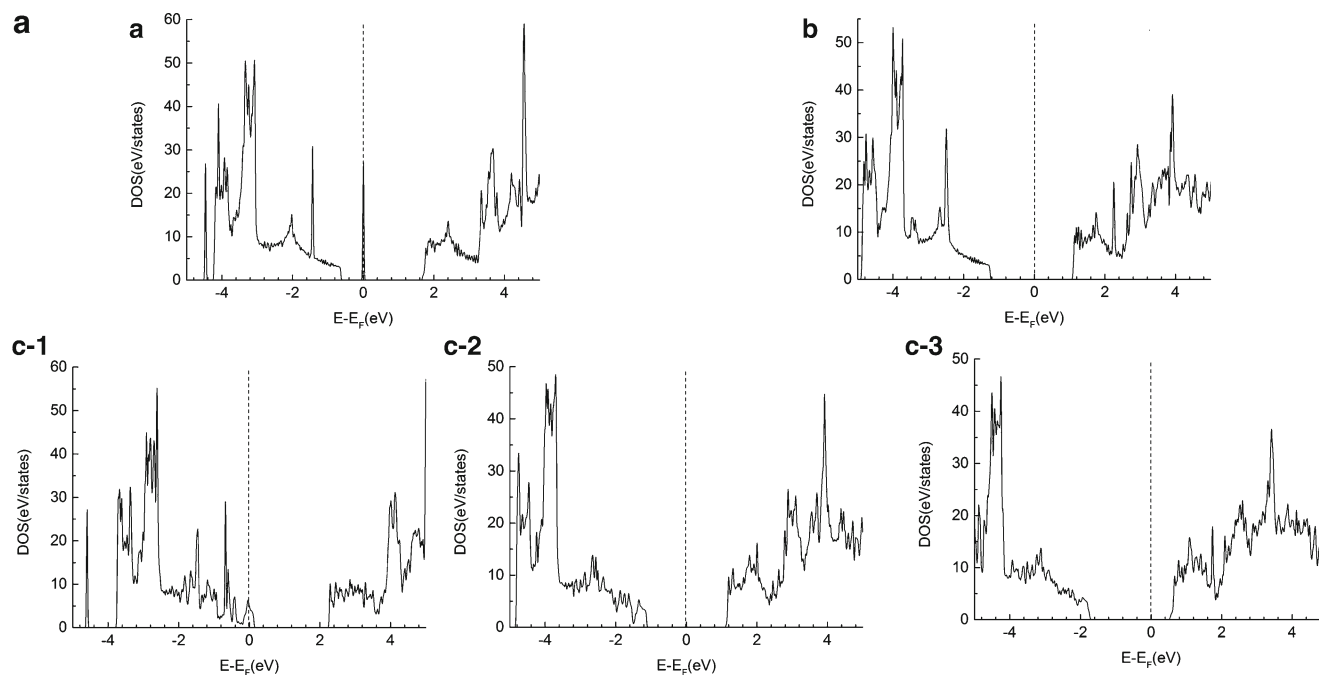


**Fig. 3** The figure depicts the total density of states (3a) and partial density of states (3b) for the 4x4 periodicity

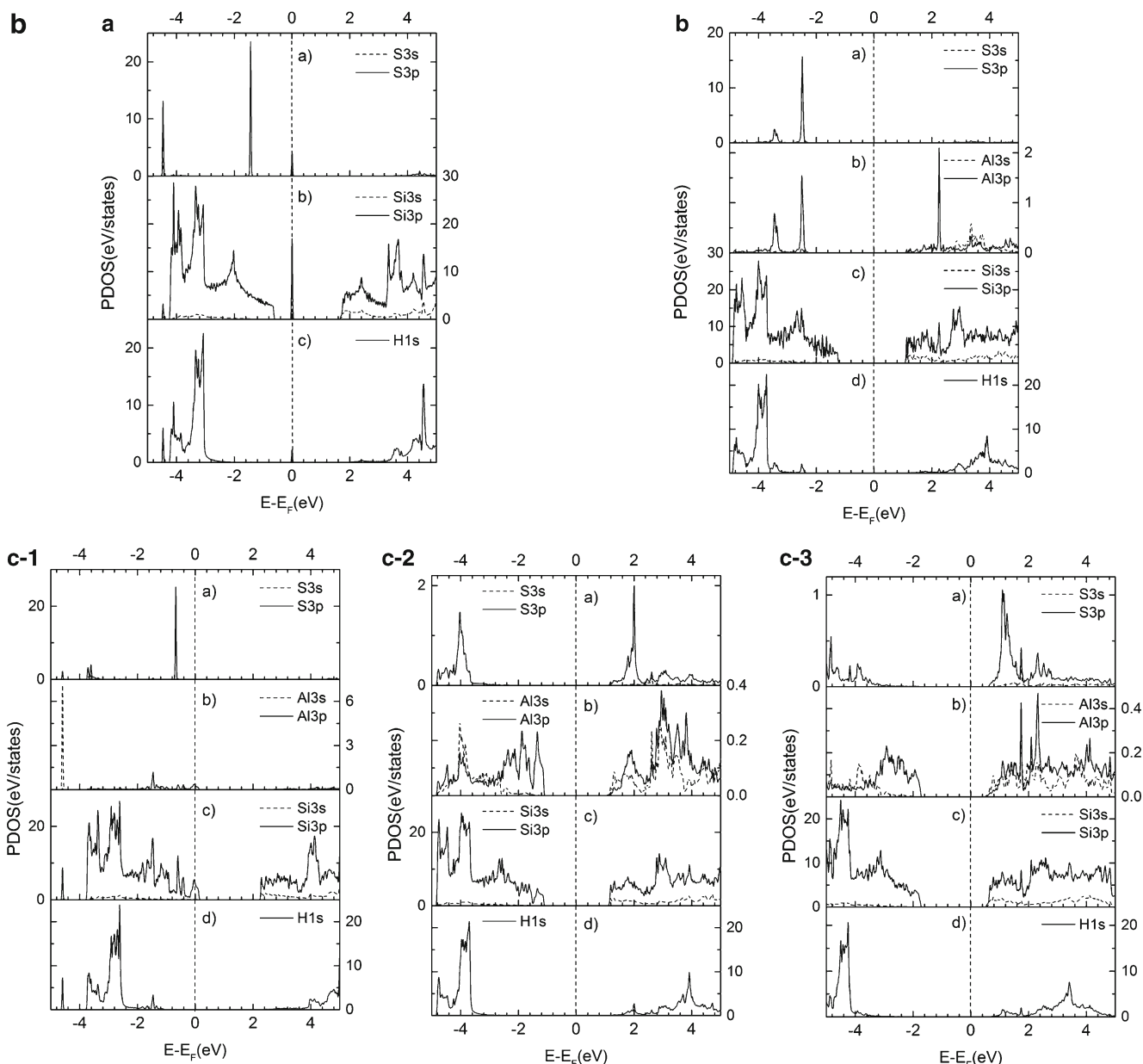


Fig. 3 (continued)

mainly formed by the S-3p, Si-3p orbitals, and Al-3p and 3s orbitals also participating. The partial DOS of the 3x3 and 2x2 periodicities exhibit similar features.

*Geometry C-2*

In panel (C-2) of Fig. 3a the total DOS for geometry C-2 is displayed in a similar fashion as presented for geometry C-1. Some structural changes with the periodicity are obtained. The energy gap shows a monotonic variation with periodicity, it decreases when the periodicity changes from 4x4 to 2x2 (from 2.2 eV to 1.75 eV). Similar to the total DOS discussed previously the structural interpretation is given in terms of the partial DOS. The total DOS is obtained with

contributions of S, Al, Si and H orbitals reported in panel (C-2) of Fig. 3b. The valence band is formed by the S-3p, Al-3s, Si-3p and H-1s orbitals, with S and Si making the most important contributions, nevertheless Al-3p orbital and the H-1s orbital are also contributing. At the conduction band, the total DOS is mainly formed by the S-3p, Si-3p orbitals, with Al-3p and 3s orbitals also participating. Similarly, PDOS of the 3x3 and 2x2 periodicities contribute to the total DOS.

*Geometry C-3*

Finally results of the DOS and partial DOS of geometry C-3 are reported. In this geometry an aluminum atom replaces a silicon atom at a lattice site in an otherwise occupied by a

saturated silicon atom in the lower monolayer. After relaxation, the aluminum has no hydrogen bonded to it and the monolayer is distorted at the vicinity of the doping site. In panel (C-3) of Fig. 3a, the total DOS for the 4x4 periodicity is displayed. The total DOS features exhibit some minor changes with the periodicity. One point to remark is that the estimated energy gap in this DFT theory do not show a monotonic behavior; it increases when the periodicity changes from 4x4 to 3x3 (2.2 to 2.25 eV) and then decreases as the aluminum concentration increases, the periodicity changes from 3x3 to 2x2 (2.25 to 1.85 eV). Total DOS features of the 4x4 periodicity are interpreted in terms of the partial DOS depicted in panel (C-3) of Fig. 3b. At the valence band, this is formed by the S-3p, Al-3p, Si-3p and H-1s orbitals, with S and Si making the most important contributions, nevertheless Al-3s orbital and the H-1s orbital are contributing. At the conduction band the total DOS is mainly composed by the S-3p, Si-3p orbitals, and Al-3p and 3s orbitals and H-1s orbital also participating. Similar features are exhibited by the partial of the 3x3 and 2x2 periodicities, results are not reported.

### Charge density

Calculations of the charge density plots of all ground state configurations are presented in Fig. 4 (A, B, C-1, C-2 and C-3). The figure displays lateral views of every case. The description of the charge distribution is focused at the vicinities of the hydrogen vacancy or at the impurity place. It is clear how the charge is distributed around every atom of

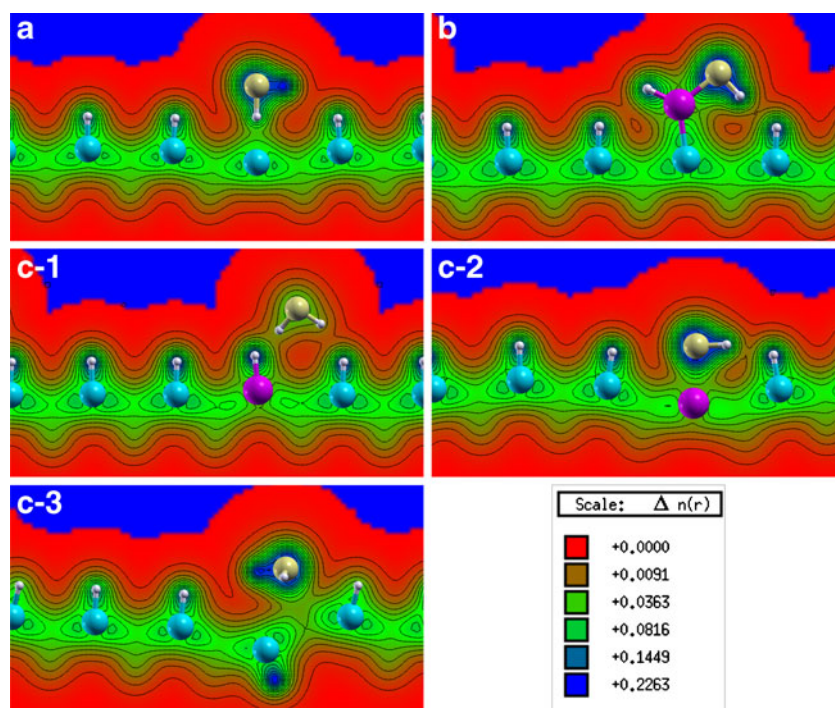
the structure. In configuration A (panel (A)) the plane of the molecule is perpendicular to the silicane layer; one hydrogen atom makes a bond with the sulfur with the bond being parallel to the layer. The other H also makes a bond with the S with the bond being perpendicular. High charge density is distributed between the H and the S atoms at the bond parallel to the layer, nevertheless charge is also present at the other bond of the molecule. Note that there is also charge between the H of the molecule and the Si at the H vacancy. This charge induces physisorption between the molecule and the silicon atom in agreement with values of the adsorption energies reported in Table 1.

The dissociated adsorption of the H<sub>2</sub>S molecule in geometry B (panel (B)) displays the structure; H-S-Al-H, with the Al atom making a bond with a silicon atom. High charge density is between the H-S bond however part of the charge is also distributed at the H-Al and Al-Si bonds. It is apparent that in this case there exist chemisorptions as also supported by the adsorption energies.

In the non dissociated adsorption of geometry C-1 (panel (C-1)) the hydrogen sulfide molecule is placed near the silicane layer. Due to the presence of Al the H atoms of the molecule are at different distances from the layer. The charge is not homogeneously distributed at the space between the molecule and the layer. According to this charge distribution it may be said that there is a weak physisorption as indicated by the value of the adsorption energy.

The charge distribution in geometry C-2 (panel (C-2)) indicates that most of the charge is at the vicinity of the H<sub>2</sub>S molecule, which is parallel to the silicane layer and near the

**Fig. 4** The side views of the charge density plots for the most stable configurations in the 4x4 periodicity is shown





aluminum. The figure also shows charge between the molecule and the aluminum. This plot exhibits the existence of chemisorptions in agreement with the adsorption energy value.

Finally, results of the charge distribution in geometry C-3 are presented. In this case, the molecule plane is not parallel to the silicane nevertheless high charge density is distributed at the vicinity of the adsorbed molecule. Note the presence of charge between the molecule and the aluminum, which yields chemisorptions in agreement with the values of the adsorption energy.

## Conclusions

First principles total energy calculations have been performed to study the hydrogen sulfide (H<sub>2</sub>S) adsorption on silicane in dissociative and non-dissociative forms. Undoped and doped silicane have been considered: The undoped structure contains a hydrogen vacancy (A) and the doped structure has been studied in two main configurations; in one case the aluminum replaces a hydrogen atom (B) and in another configuration the aluminum replaces a silicon atom at a lattice site (C-1, C-2 and C-3 geometries). All calculations consider three supercells; 4x4, 3x3 and 2x2. The non-dissociative adsorption takes place in geometries (A), (C-1), (C-2) and (C-3) while the dissociative in (B). Binding energies indicate chemisorptions in geometries (B), (C-2) and (C3), while physisorption in (A) and (C-1). The presence of the doping produces some electronic changes as the periodicity varies. Calculations of the total density of states (DOS) indicate that in most cases the energy gap decreases as the periodicity changes from 4x4 to 2x2. Features of the total DOS have been explained in terms of the partial DOS. In geometry (A) the total DOS at the valence band is formed by the Si-3p, S-3p and H-1s orbitals while at the conduction band the contributions come from Si-3p and H-1s orbitals. In all other cases at both valence and conduction bands, the main contributions to the total DOS come from the 3p orbitals of Si, Al and S, and from the 1s orbital of H. Charge density plots explain quite well the chemisorptions and physisorptions of the molecule on silicane in agreement with adsorption energies.

**Acknowledgments** We wish to acknowledge the partial financial support of projects: Cuerpo Académico Física Computacional de la Materia Condensada (BUAP-CA-194) and VIEP-BUAP-EXC11-G. We are also grateful to the technical assistance of L. Rojas and N. Mendes at the computer center, in the Instituto de Física “Luis Rivera Terrazas” of the Universidad Autónoma de Puebla (IFUAP).

## References

- Çakmak M, Srivastava GP (1998) Ab initio study of atomic geometry, electronic states, and bonding for H<sub>2</sub>S adsorption on III-V semiconductor (110)-(1×1) surfaces. *Phys Rev B* 57:4486–4492. doi:10.1103/PhysRevB.57.4486
- Çakmak M, Srivastava GP (1999) Adsorption of partially and fully dissociated H<sub>2</sub>S molecules on the Si(001) and Ge(001) surfaces. *Phys Rev B* 60:5497–5505. doi:10.1103/PhysRevB.60.5497
- Russell SM, Liu D-J, Kawai M, Kim Y, Thiel PA (2010) Low-temperature adsorption of H<sub>2</sub>S on Ag(111). *J Chem Phys* 133:124705–124713. doi:10.1063/1.3481481
- Jayaraman V, Mangamma G, Gnanasekaran T, Periaswami G (1996) Evaluation of BaSnO<sub>3</sub> and Ba(Zr,Sn)O<sub>3</sub> solid solutions as semiconductor sensor materials. *Solid State Ionics* 86–88:1111–1114. doi:10.1016/0167-2738(96)00277-9
- Akimov BA et al. (1997) The electrical conductivity of polycrystalline SnO<sub>2</sub>(Cu) films and their sensitivity to hydrogen sulfide. *Semiconductors* 31:335–339. doi:10.1134/1.1187182
- Schutt HU, Rhodes PR (1996) Corrosion in an aqueous hydrogen sulfide, ammonia, and oxygen system. *Corrosion* 52(12):947–952. doi:10.5006/1.3292088
- Conrad S, Mullins DR, Xin QS, Zhu XY (1996) Thermal and photochemical deposition of sulfur on GaAs(100). *Appl Surf Sci* 107:145–152. doi:10.1016/S0169-4332(96)00499-0
- Jiang DE, Carter EA (2005) First principles study of H<sub>2</sub>S adsorption and dissociation on Fe(110). *Surf Sci* 583:60–68. doi:10.1016/j.susc.2005.03.023
- Ren C, Wang X, Miao Y, Yi L, Jin X, Tan Y (2010) DFT study of the dissociative adsorption of H<sub>2</sub>S molecule on the Si(1 1 1)-7×7 surface. *J Mol Struct (THEOCHEM)* 949:96–100. doi:10.1016/j.theochem.2010.03.014
- Fujiwara K (1981) Electron orbital energies of H<sub>2</sub>S and H<sub>2</sub>O chemisorbed on the Si(111) 7×7 surface. *J Chem Phys* 75:5172–5179. doi:10.1063/1.441867
- Rezaei MA, Stipe BC, Ho W (1998) Atomically resolved determination of the adsorption sites as a function of temperature and coverage: H<sub>2</sub>S on Si(111)-(7×7). *J Phys Chem B* 102(52):10941–10947. doi:10.1021/jp983207b
- Rezaei MA, Stipe BC, Ho W (1998) Inducing and imaging single molecule dissociation on a semiconductor surface: H<sub>2</sub>S and D<sub>2</sub>S on Si(111)-7×7. *J Chem Phys* 109:6075–6078. doi:10.1063/1.477233
- Chakarov DV, Ho W (1995) Thermal and photo-induced desorption, dissociation, reactions of H<sub>2</sub>S adsorbed on Si(111) 7×7. *Surf Sci* 323:57–70. doi:10.1016/0039-6028(94)00661-X
- Novoselov KS et al. (2005) Two-dimensional atomic crystals. *Proc Natl Acad Sci USA* 102:10451–10453. doi:10.1073/pnas.0502848102
- Novoselov KS et al. (2005) Two-dimensional gas of massless Dirac fermions in graphene. *Nature* 438:197–200. doi:10.1038/nature04233
- Lebègue S, Eriksson O (2009) Electronic structure of two-dimensional crystals from ab initio theory. *Phys Rev B* 79:115409–115413. doi:10.1103/PhysRevB.79.115409
- Hussain T et al. (2011) Ab initio study of lithium-doped graphene for hydrogen storage. *EPL* 96:27013–27017. doi:10.1209/0295-5075/96/27013
- Hussain T, Pathak B, Ramzan M, Maark TA, Ahuja R (2012) Calcium doped graphene as a hydrogen storage material. *Appl Phys Lett* 100:183902–183907. doi:10.1063/1.4710526
- Houssa M, Pourtois G, Afanas'ev VV, Stesmans A (2010) Can silicon behave like graphene? A first-principles study. *Appl Phys Lett* 97:112106–112109. doi:10.1063/1.3489937
- Houssa M, Scalise E, Sankaran K, Pourtois G, Afanas'ev VV, Stesmans A (2011) Electronic properties of hydrogenated silicene and germanene. *Appl Phys Lett* 98:223107–223110. doi:10.1063/1.3595682
- Lew Yan Voon LC, Sandberg E, Aga RS, Farajian AA (2010) Hydrogen compounds of group-IV nanosheets. *Appl Phys Lett* 97:163114–163117. doi:10.1063/1.3495786
- Şahin H, Cahangirov S et al. (2009) Monolayer honeycomb structures of group-IV elements and III-V binary compounds: First-principles calculations. *Phys Rev B* 80:155453–155465. doi:10.1103/PhysRevB.80.155453

23. Cahangirov S, Topsakal M, Aktürk E, Şahin H, Ciraci S (2009) Two- and one-dimensional honeycomb structures of silicon and germanium. *Phys Rev Lett* 102:236804–236808. doi:10.1103/PhysRevLett.102.236804
24. Wang S (2010) Studies of physical and chemical properties of two-dimensional hexagonal crystals by first-principles calculation. *J Phys Soc Jpn* 79:064602–064607. doi:10.1143/JPSJ.79.064602
25. Kara A et al. (2009) Physics of silicene stripes. *J Supercond Nov Magn* 22:259–263. doi:10.1007/s10948-008-0427-8
26. Aufray B et al. (2010) Graphene-like silicon nanoribbons on Ag(110): a possible formation of silicene. *Appl Phys Lett* 96:183102–183105. doi:10.1063/1.3419932
27. Padova DE, Quaresima C et al. (2011) sp<sup>2</sup>-like hybridization of silicon valence orbitals in silicene nanoribbons. *Appl Phys Lett* 98:081909–081912. doi:10.1063/1.3557073
28. Guzmán-Verri GG, Lew Yan Voon LC (2011) Band structure of hydrogenated Si nanosheets and nanotubes. *J Phys Condens Matter* 23:145502–145507. doi:10.1088/0953-8984/23/14/145502
29. Cheng YC, Zhu ZY, Schwingenschlögl U (2011) Doped silicene: evidence of a wide stability range. *EPL* 95:17005–17010. doi:10.1209/0295-5075/95/17005
30. Takeda K, Shiraishi K (1989) Electronic structure of Si-skeleton materials. *Phys Rev B* 39:11028–11037. doi:10.1103/PhysRevB.39.11028
31. Van de Walle CG, Northrup JE (1993) First-principles investigation of visible light emission from silicon-based materials. *Phys Rev Lett* 70:1116–1119. doi:10.1103/PhysRevLett.70.1116
32. Nakano H et al. (2006) Soft synthesis of single-crystal silicon monolayer sheets†. *Angew Chem* 118(38):6451–6454. doi:10.1002/ange.200600321
33. Dahn JR, Way BM, Fuller E (1993) Structure of siloxene and layered polysilane (Si<sub>6</sub>H<sub>6</sub>). *Phys Rev B* 48:17872–17877. doi:10.1103/PhysRevB.48.17872
34. Soler JM, Artacho E, Gale JD (2002) The SIESTA method for ab initio order-N materials simulation. *J Phys Condens Matter* 14:2745–2779. doi:10.1088/0953-8984/14/11/302
35. Ordejon P, Artacho E, Soler JM (1996) Self-consistent order-N density-functional calculations for very large systems. *Phys Rev B* 53:10441–10444. doi:10.1103/PhysRevB.53.R10441
36. Perdew JP, Burke K, Ernzerhof M (1996) Generalized gradient approximation made simple. *Phys Rev Lett* 77:3865–3868. doi:10.1103/PhysRevLett.77.3865
37. Hamann DR, Schlüter M, Chiang C (1979) Norm-conserving pseudopotentials. *Phys Rev Lett* 43:1494–1497. doi:10.1103/PhysRevLett.43.1494
38. Bachelet GB, Hamann DR, Schlüter M (1982) Pseudopotentials that work: from H to Pu. *Phys Rev B* 26:4199–4228. doi:10.1103/PhysRevB.26.4199
39. Kleinman L, Bylander DM (1982) Efficacious form for model pseudopotentials. *Phys Rev Lett* 48:1425–1428. doi:10.1103/PhysRevLett.48.1425
40. Junquera J, Paz Ó, Sánchez-Portal D, Artacho E (2001) Numerical atomic orbitals for linear-scaling calculations. *Phys Rev B* 64:235111–235120. doi:10.1103/PhysRevB.64.235111
41. Monkhorst HJ, Pack JD (1976) Special points for Brillouin-zone integrations. *Phys Rev B* 13:5188–5192. doi:10.1103/PhysRevB.13.5188
42. Edwards TH, Moncur NK, Snyder LE (1967) Ground-state molecular constants of hydrogen sulfide. *J Chem Phys* 46:2139–2142. doi:10.1063/1.1841014
43. Lai Y-H, Yeh C-T, Lin Y-H, Hung W-H (2002) Adsorption and thermal decomposition of H<sub>2</sub>S on Si(100). *Surf Sci* 519:150–156. doi:10.1016/S0039-6028(02)02208-2
44. Dominic RA (2008) First-principles studies of H<sub>2</sub>S adsorption and dissociation on metal surfaces. *Surf Sci* 602:2758–2768. doi:10.1016/j.susc.2008.07.001
45. Jiang DE, Carter EA (2004) Adsorption, diffusion, and dissociation of H<sub>2</sub>S on Fe(100) from first principles. *J Phys Chem B* 108:19140–19145. doi:10.1021/jp046475k
46. Leenaerts O, Partoens B, Peeters FM (2009) Water on graphene: hydrophobicity and dipole moment using density functional theory. *Phys Rev B* 79:235440. doi:10.1103/PhysRevB.79.235440